

## A HYBRID APPROACH FOR FAULT DIAGNOSIS OF SPUR GEARS USING HU INVARIANT MOMENTS AND ARTIFICIAL NEURAL NETWORKS

F. Michael Thomas Rex<sup>1)</sup>, A. Andrews<sup>1)</sup>, A. Krishnakumari<sup>2)</sup>,  
P. Hariharasakthisudhan<sup>1)</sup>

1) National Engineering College, Department of Mechanical Engineering, Kovilpatti – 628 503, Tamil Nadu, India  
(✉ [michealrex@hotmail.com](mailto:michealrex@hotmail.com), +91 948 626 4631 [andrewsnzj@gmail.com](mailto:andrewsnzj@gmail.com), [harimeed2012@gmail.com](mailto:harimeed2012@gmail.com))

2) Hindustan Institute of Technology and Science, Department of Mechanical Engineering, Chennai – 603103, Tamil Nadu, India ([a\\_krishnakumari@yahoo.co.in](mailto:a_krishnakumari@yahoo.co.in))

### Abstract

Achieving a reliable fault diagnosis for gears under variable operating conditions is a pressing need of industries to ensure productivity by averting unwanted breakdowns. In the present work, a hybrid approach is proposed by integrating Hu invariant moments and an artificial neural network for explicit extraction and classification of gear faults using time-frequency transforms. The Zhao-Atlas-Marks transform is used to convert the raw vibrations signals from the gears into time-frequency distributions. The proposed method is applied to a single-stage spur gearbox with faults created using electric discharge machining in laboratory conditions. The results show the effectiveness of the proposed methodology in classifying the faults in gears with high accuracy.

Keywords: gear fault, Zhao-Atlas-Marks, time-frequency domain features, Hu invariant moments, ANN.

© 2020 Polish Academy of Sciences. All rights reserved

## 1. Introduction

Gears are the essential components of industrial machinery and often subjected to wear and impact damages due to their high load-carrying capacity. The failure of the gear may cause an unnecessary shutdown that leads to substantial economic losses. Therefore, the condition monitoring of the gears is inevitable in ensuring the reliability of the system. Many research works have been contributed to condition monitoring of gears by extracting gear fault information from the vibration signals.

Vibration amplitude-based fault identification techniques in gears are inefficient for non-stationary signals extracted from the faulty gear system. The non-stationary signals are properly treated by the time-frequency domain analysis [1]. *Short-time Fourier transform* (STFT), *wavelet transform* (WT) and *Wigner-Ville distribution* (WVD) are commonly used to convert the non-stationary signals into a time-frequency domain [2, 3]. Urbanek *et al.* [4] compared the

effectiveness of various frequency domain-based signal processing techniques for detecting the faults in a roller bearing. They have concluded that the method using spectral coherence for narrowband envelope analysis was found to be effective in detecting the faults. Zimroz [5] performed a time-frequency analysis to measure the instantaneous shaft speed of the wind turbine gearbox. The gear fault identification based on Hilbert-Hung transform was proposed to overcome the problem of reconstructing a feature matrix of singular value decomposition [6]. Recently, *Zhao-Atlas-Marks* (ZAM) transforms are used to analyse the short-range time-frequency distribution of vibration signals precisely. The ZAM distribution exhibited excellent frequency resolution and sharp energy concentration [7]. Sun *et al.* [8] developed a novel signal processing technique based on structured sparsity time-frequency analysis to identify defects in gears. Zhang *et al.* [9] developed a fault diagnosis method based on the *Lucy-Richardson Deconvolution* (LRD). The LRD based method identified the fault frequencies in gears and bearing to detect faults. Afia *et al.* [10] applied a robust signal processing technique that uses Autogram to extract the fault signature from vibration signals of gears. Guan *et al.* [11] proposed a method for gearbox fault diagnosis using velocity synchronous Fourier transform and order analysis. This method reduced the interpolation errors that often occurred in the conventional resampling based order tracking methods.

Hybrid statistical analysis with feature extraction and classification methods are employed by a few researchers to identify the defects in the machinery. Juan *et al.* [12] proposed a diagnosis methodology to find the wear defect in gears using the Fisher score analysis, linear discriminant analysis and a fuzzy classifier. Krishnakumari *et al.* [13] used a decision tree and fuzzy classifier for fault classification of spur gears. They have extracted the statistical features from the vibration signal and used them for constructing a decision tree. Dhamande and Chaudhari [14] proposed a fault feature extraction technique for gear fault identification. They evaluated the statistical features like standard deviation, variance and absolute maximum from Continuous and Discrete Wavelet Transforms and found improvement in the accuracy of fault classification. The *support vector machine* (SVM) for feature extraction in gear fault diagnosis was found to be insensitive to varying operating conditions and useful to enhance classification accuracy. Zhang *et al.* [15] implemented an integrated technique using Empirical Mode Decomposition and SVM for gear fault diagnosis. Vamsi *et al.* [16] developed a condition monitoring technique to determine a fault in a wind turbine gearbox. They have used wavelet analysis to extract the features from the signals and the SVM technique was used as a feature classification technique. A decision tree algorithm was used to select the dominant features from the extracted statistical features.

An *Artificial Neural Network* (ANN) is a reliable tool for dataset classification and it has been successfully used in previous studies for fault classification of the rotating machinery. Saravanan and Ramachandran [17] applied wavelet transform and an ANN to identify the defects in the gearbox. They have extracted wavelet features from the signals and fed them as input to the neural network. The results have shown that the neural networks are very accurate in identifying the faults. Wang and Liao [18] proposed a gear fault diagnosis tool using Bayesian neural networks that provides an effective diagnosis, while the input information is uncertain and incomplete. The statistical factors of vibration signals in the time-domain were used to train the network. Dworakowski *et al.* [19] developed an ANN-based diagnosis technique to detect the defects in epicyclic gearboxes. The extracted multi-dimensional features were used for training the ANN.

The literature reveals that the need for evolution of signal processing and feature extraction techniques is inevitable to improve the effectiveness of fault identification in gears. Further, the extraction of nonlinear features that provide critical information about the gear defects from the

non-stationary vibration signal is still found to be challenging. The aim of this research work is to present a novel hybrid approach for gear fault detection and classification. The research work investigates the use of the Hu invariants and the ANN as a tool for feature extraction and subsequent classification of gear faults. Further, it also highlights the effectiveness of the proposed approach with the experimental study.

## 2. Proposed methodology

The overall procedure of the proposed methodology is illustrated in Fig. 1. Initially, an experimental setup was developed to simulate gear faults. The vibration signals were acquired using an accelerometer and a signal analyser from the gear fault simulator corresponding to various gear faults. Consequently, a ZAM transform was applied to convert raw signals into a time-frequency distribution. Further, Hu moments were adopted to extract the features from the time-frequency distribution to enhance the fault prediction. Finally, the extracted features were used to train the ANN and the validated ANN model was used to classify the gear faults automatically.

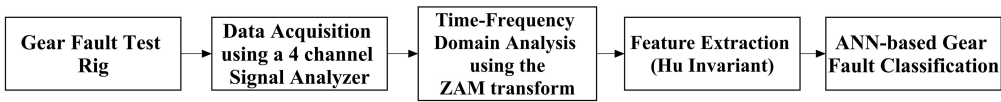


Fig. 1. Flow diagram of fault diagnosis of gear using Hu moments.

## 3. Experimental setup

The experimental test rig consists of a single-stage spur gearbox, which possesses two parallel shafts and two spur gears, is shown in Fig. 2. The gears are made up of EN 24 steel with a 5 mm

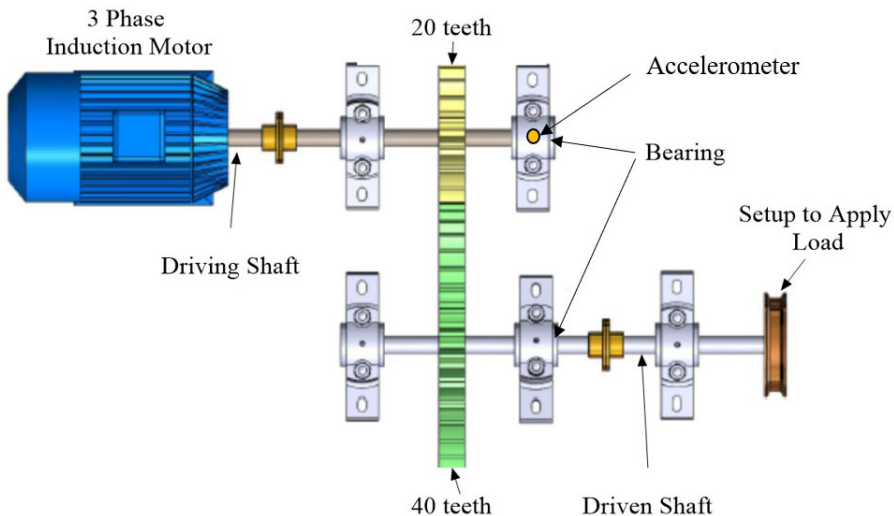
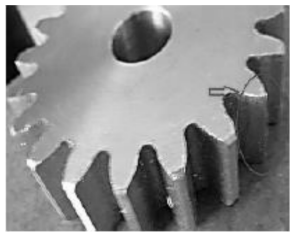


Fig. 2. The gearbox fault simulator.

module and 20° pressure angle involute teeth. The driving shaft of the gearbox is connected to a three-phase induction motor through a love-joy coupling. The driven shaft of the gearbox is connected to a setup to apply the load through another love-joy coupling. A piezoelectric accelerometer (IEPE) is mounted on the bearing housing to collect the vibration signal as shown in Fig. 2. Vibration data were collected using a four-channel acquisition system (NI 9233). The speed of the motor is varied using a variable frequency drive.

In this study, three defective pinions were used for collecting vibration signals. The details of defective gears are shown in Table 1. The various defects were artificially created in the pinions using Electric Discharge Machining. In order to represent the worn-out tooth, a depth of 1 mm was removed on either side of a tooth along the flank face in the axial direction of gear. The gear with a broken tooth was obtained by cutting a portion of the gear tooth with a plane oriented in a corner edge of the gear tooth. The cutting plane can be represented by projecting a line passing through the coordinates located at a distance of 2 mm depth from the top land and 6 mm along face width at a gear tooth corner.

Table 1. Detail of pinions.

Defects	Pinion without defects	Pinion with worn-out tooth	Pinion with broken tooth
Image of defective pinion			

Initially, the speed of the motor was set to 400 rpm using the variable frequency drive. The defect-free pinion was connected to the gearbox and the vibration signals were collected from the accelerometer through the data acquisition system and recorded. The sampling rate was set as 2048 samples/second. Subsequently, the pinion was replaced with pinions with defects and the data from the signals were recorded. A set of data was also recorded by applying a load of 100 N for the case of the pinion with a broken tooth. The vibration signals for the undamaged and damaged pinions were illustrated in Fig. 3. By comparing the signals, a little periodic modulation characteristic was observed for the reference signal shown in Fig. 3a. Whereas, a series of impulsive responses were observed for the fault conditions illustrated in Figs. 3b, 3c and 3d. Further, the observed trend was also validated by determining the kurtosis value for the signals. The kurtosis value for the pinion without defects was found to be 2.7. The pinions with defects such as a worn-out tooth, broken tooth and broken tooth under load were calculated as 4.3, 4.7 and 5.1 respectively.

Further, the recorded signals were imported into the MATLAB software for converting raw data into time-frequency transform using the ZAM transform. Consequently, Hu moments were determined for the ZAM transform to extract the features of the faults.

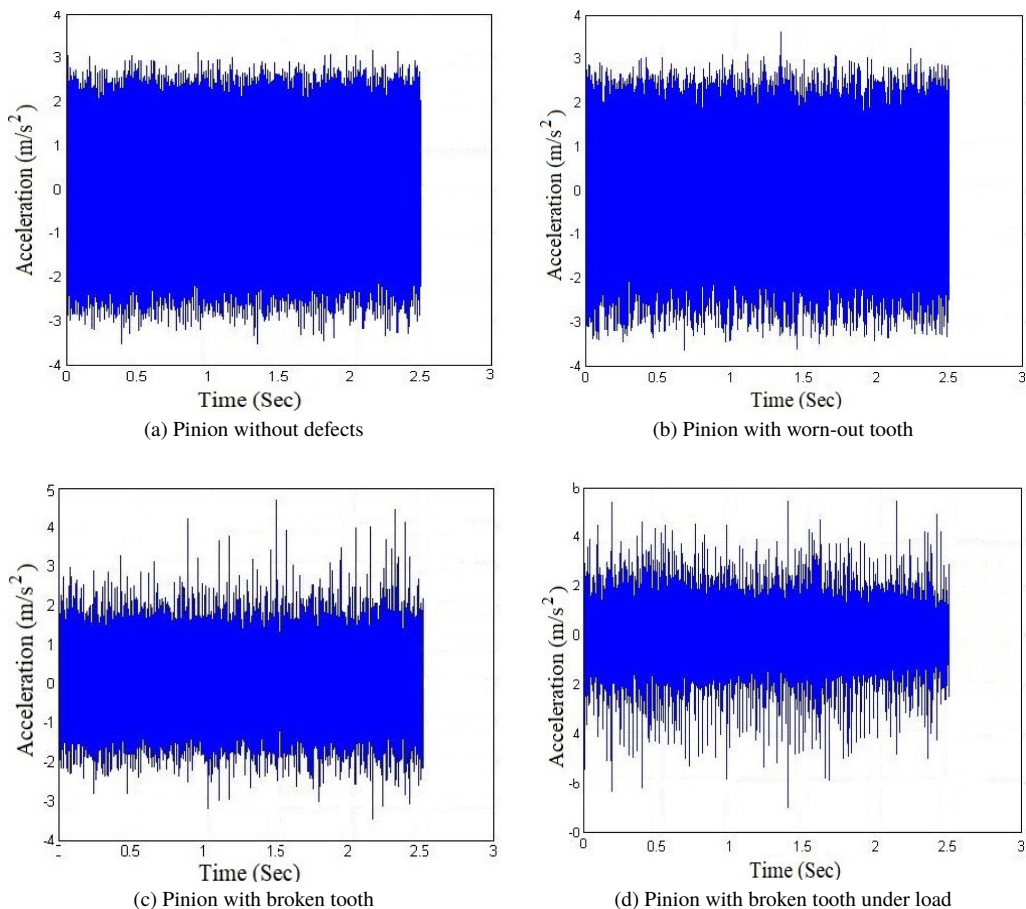


Fig. 3. Vibration signals from pinions under various fault conditions.

#### 4. Signal processing and feature extraction

Signal processing techniques enable effective early fault detection by analysing the raw vibration signal. They must be capable of decomposing the signals that are nonlinear and non-stationary due to the defects and various loading conditions. The presence of faults in the rotary system increases the nonlinearity of the vibration signal. Feature extraction techniques allow to extract the information about faults from the decomposed signals. The results of applying the ZAM transform to process the signals and Hu invariant moments to extract features from the decomposed signals are presented in the following section.

##### 4.1. Zhao-Atlas-Marks transform (ZAM)

The ZAM transform distributes the energy of the signals over time and frequency as it is an energy distribution. Furthermore, it is a powerful time-frequency analysis tool [20] for fault identification and diagnosis. The frequency resolution and energy concentration of the ZAM transform is observed to be better than that of the STFT and other time-frequency transforms.

Further, ZAM can resolve non-stationary signals. Cohen’s Class Time-Frequency Distributions are a generalized form of phase-space distribution and the other time-frequency distributions are derived from it. The general form of Cohen’s class of distribution [20] for a signal  $f(t)$  is presented in equation (1). In the equation,  $\varphi(\varepsilon, \tau)$  is the kernel that defines the time-frequency transformation

$$D(t, \omega; \mu) = \iiint e^{j(\varepsilon\mu - \tau\omega - \varepsilon t)} \varphi(\varepsilon, \tau) f(\mu + \tau/2) f(\mu - \tau/2) d\mu d\tau d\varepsilon, \tag{1}$$

where,  $t$  – instantaneous time,  $\omega$  – instantaneous frequency,  $\tau$  – running time,  $\varepsilon$  – frequency,  $\mu$  – position variables used in the integration.

The development of the ZAM “cone kernel” was intended to introduce finite time support and reduce cross-terms [21]. The kernel equation is defined in equation (2).

$$\varphi(\varepsilon, \tau) = \frac{\varphi_1(\tau) \sin(\varepsilon|\tau|/a)}{\varepsilon/2}, \tag{2}$$

$\varphi_1(\tau)$  is a function to be specified and the parameter ‘ $a$ ’ value is taken as 1 [20]. The ZAM distribution is obtained by substituting the kernel equation (2) in Cohen’s class of distribution.

#### 4.2. Feature extraction using Hu invariant moments

The Hu moments are used to characterize visual patterns in images [22]. The set of moments for different images is found to be unique and useful in the classification of images [23]. The Hu moments are derived from the geometric moments of an image. The image moments are a weighted average of image pixel intensities. The pixel intensity of an image (I) at an orientation (x,y) is given by  $I(x,y)$ . The moment (M) of the image is calculated by determining the summation of all pixel intensities in the image (I) and given in equation (3).

$$M = \sum_x \sum_y I(x, y). \tag{3}$$

In equation (3), the pixel intensities are weighted only based on their intensity and irrespective of their location in the image. The equation is revised by considering the intensity of the pixels and their location in the image and presented in equation (4).

$$M_{i,j} = \sum_i \sum_j x^i y^j I(x, y), \tag{4}$$

where  $i, j = 0, 1, 2, 3, \dots$

The central moments ( $\mu_{ij}$ ) of the image are obtained by subtracting off the centroid ( $\bar{x}\bar{y}$ ) from  $x$  and  $y$  in the moment equation (4) and presented in equation (5).

$$\mu_{ij} = \sum_i \sum_j (x - \bar{x})^i (y - \bar{y})^j I(x, y), \tag{5}$$

$$\bar{x} = \frac{M_{10} \text{ (Sum of } x \text{ coordinates of the pixel in image)}}{M_{00} \text{ (Area of the image)}}, \tag{6}$$

$$\bar{y} = \frac{M_{01} \text{ (Sum of } y \text{ coordinates of the pixel in image)}}{M_{00} \text{ (Area of the image)}}. \tag{7}$$

In feature extraction, the moments must be invariant to translation, scale, and rotation for pattern recognition. The central moments are invariant with respect to position. In order to make the moments invariant to scaling, the normalized central moments ( $\eta_{ij}$ ) of the image are determined using the equation (8).

$$\eta_{ij} = \frac{\mu_{ij}}{\mu_{00}^{\left(1 + \frac{i+j}{2}\right)}}. \quad (8)$$

The Hu moments are a set of seven moments [23] which are nonlinear combinations of normalized central moments ( $\eta_{ij}$ ). The seven Hu moments are given in equations (9)–(15).

$$h_1 = \eta_{20} + \eta_{02}, \quad (9)$$

$$h_2 = (\eta_{20} - \eta_{02})^2 + 4\eta_{11}^2, \quad (10)$$

$$h_3 = (\eta_{30} - \eta_{12})^2 + (\eta_{03} - 3\eta_{21})^2, \quad (11)$$

$$h_4 = (\eta_{30} + \eta_{12})^2 + (\eta_{03} + 3\eta_{21})^2, \quad (12)$$

$$h_5 = (3\eta_{30} - 3\eta_{12})(\eta_{30} + \eta_{12}) \left[ (\eta_{30} + \eta_{12})^2 - 3(\eta_{21} + \eta_{03})^2 \right] + (3\eta_{21} - \eta_{03})(\eta_{21} + \eta_{03}) \left[ 3(\eta_{30} + \eta_{12})^2 - (\eta_{21} + \eta_{03})^2 \right], \quad (13)$$

$$h_6 = (\eta_{20} - \eta_{02})^2 \left[ (\eta_{30} + \eta_{12})^2 - (\eta_{21} + \eta_{03})^2 \right] + 4\eta_{11}(\eta_{30} + \eta_{12}) + (\eta_{21} + \eta_{03}), \quad (14)$$

$$h_7 = (3\eta_{21} - \eta_{03})(\eta_{30} + \eta_{12}) \left[ (\eta_{30} + \eta_{12})^2 - (\eta_{21} + \eta_{03})^2 \right] + (3\eta_{12} - \eta_{30})(\eta_{21} + \eta_{03}) \left[ 3(\eta_{30} + \eta_{12})^2 - (\eta_{21} + \eta_{03})^2 \right]. \quad (15)$$

In the present work, Hu invariant moments are used to extract features from the time-frequency image of the ZAM transform to identify the gear faults.

### 4.3. Fault diagnosis using the ZAM transform

The measured time-domain signal was converted into a time-frequency signal using the ZAM transform as illustrated in Fig. 4. The *gear mesh frequency* (GMF) was calculated as 0.13 kHz by multiplying the number of teeth with rotational frequency. For the “healthy” gear, the energy concentration was observed at 0.11 kHz, as shown in Fig. 4a which is below the GMF. Further, it was observed from Figs. 4b and 4c that energy concentration was found to be higher than the GMF. It revealed that the gears were in a faulty condition. In contrast to the above cases, energy concentration for the gear with a broken tooth under load was found to be unclear as it exhibited energy-smear regions in the image as indicated in Fig. 4d. The actual energy concentration is also shown in Fig. 4d and it is observed to be higher than the GMF.

The ambiguities in the manual prediction of gear fault from the ZAM transform and the need for automated fault classification of gears demands a superior pattern extraction and classification technique. In the present work, the Hu invariant moments are used to extract the precise information from the ZAM transform about the faults using the equations (9)–(15). A total number of 15 sets of Hu invariant moments ( $h_1, h_2, h_3, h_4, h_5, h_6$  and  $h_7$ ) are extracted for each condition of gears at various time intervals of the signals measured. Fig. 5 shows the extracted Hu moments that are used to train the ANN for automatic fault detection.

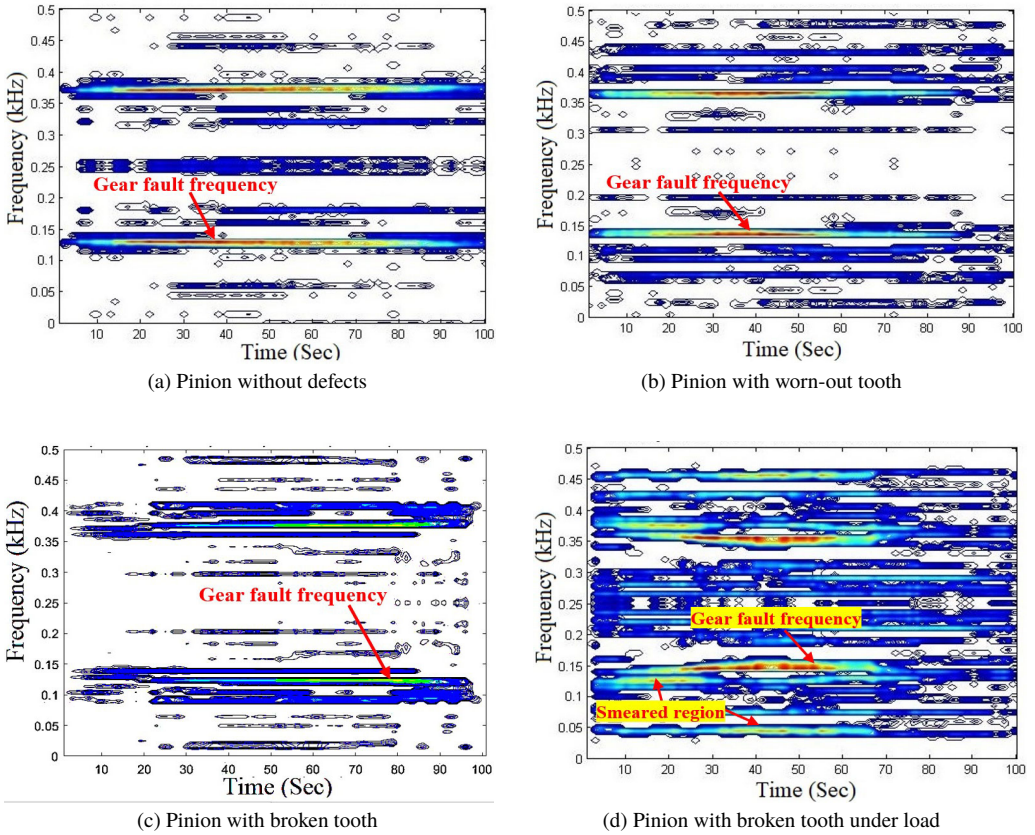


Fig. 4. ZAM Transform of the measured signals in the time-frequency domain.

## 5. Prediction of gear faults using an ANN

The effective pattern classification is inevitable for fault identification. The ANN is a proven tool for fault classification and widely used for automated fault detection and diagnosis of machine conditions. The ANN consists of an input layer, an output layer and hidden layers. The number of neurons in the input and output layer is equal to that of the number of input and output variables. In the present work, the Hu moments ( $h_1, h_2, h_3, h_4, h_5, h_6$  and  $h_7$ ) of the time-frequency transform are considered as inputs and the corresponding defects of the gear are the outputs. The output for the time-frequency feature considered for each fault is presented in Table 2.

Table 2. Output in ANN for gear faults.

S. No	Gear Faults	Output in ANN
1	Pinion without defects	0
2	Pinion with worn-out tooth	1
3	Pinion with broken tooth	2
4	Pinion with broken tooth under load	3

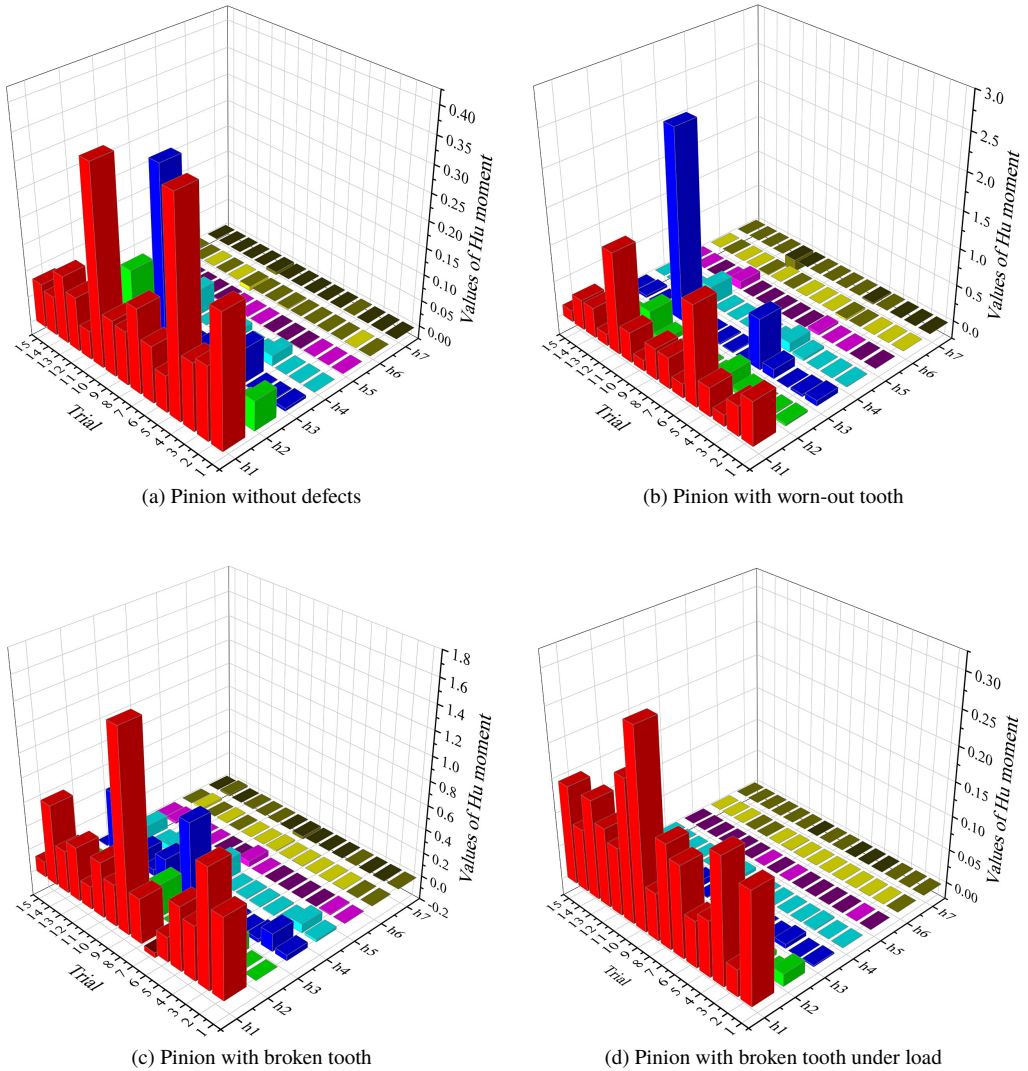


Fig. 5. Extracted features of gear conditions using Hu moments.

The number of hidden layers and the number of neurons in each hidden layer influence the prediction accuracy of an ANN. However, they may not be determined through standard procedures. Hence, various training trials are performed through varying the number of hidden layers and neurons in the hidden layer to minimize the *Mean Square Error* (MSE) as illustrated in Fig. 6. The MSE is defined as the mean of the differences between the output and the target value of fault classification during the ANN training. It can be interpreted from the Fig. 6 that the two hidden layers outperform the prediction accuracy of the single hidden layer network. Further, can be understood from Fig. 6 that the two hidden layers with seven neurons yield the minimum MSE as it increases the prediction ability of the ANN. Consequently, the network structure is fixed to two hidden layers with seven neurons in each layer. The ANN architecture for predicting gear faults is illustrated in Fig. 7.

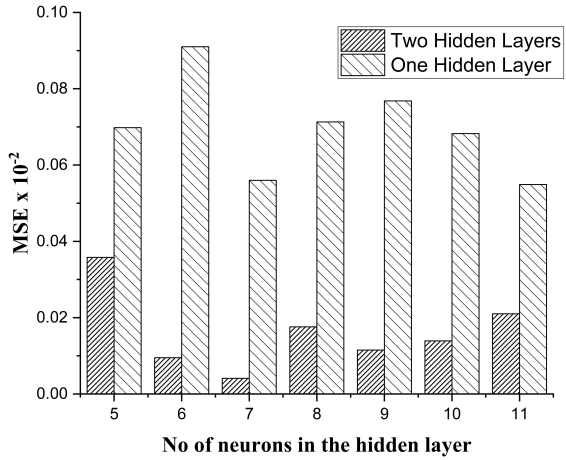


Fig. 6. MSE vs number of neurons in the hidden layer.

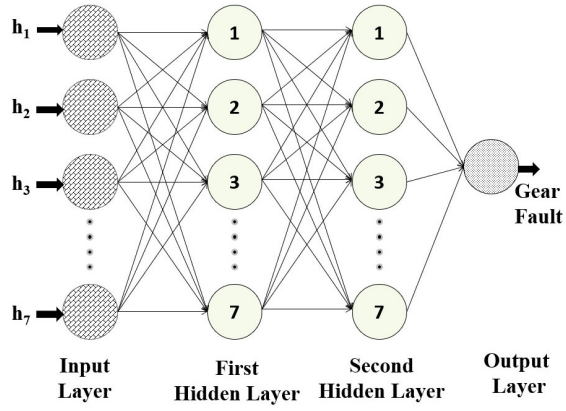


Fig. 7. The architecture of the ANN in fault classification.

**5.1. Training of the ANN**

A *Feed Forward Back Propagation* (FFBP) neural network is employed to train the ANN. In the FFBP, the input parameters are applied to the input layer that propagates into the output layer through the hidden layer using a transfer function through assigning initial weights. Based on the error between the output and the target value, the weights are adjusted from the output to the input layer and it is termed backpropagation.

In general, the ANN module is to be trained with available experimental results as input values in order to predict the results of a new set of parameters. In the present work, a total number of 60 extracted features from the ZAM transform are used to train the ANN. In the FFBP, the ANN is trained to achieve the predetermined MSE by performing various trials called epochs. The MSE of 0.00001 is set as the goal of the training process. The training process is terminated if the goal is achieved or the maximum number of epochs (trials) reached. The plot showing the convergence of the MSE with a number of epochs is presented in Fig. 8. The value of 0.0000106

was obtained as the MSE error after 69999 trials. The plot indicated a gradual decrease in the MSE and it was almost flattened out at the end. Hence, it was understood that the training was sufficient for developing an effective predictive model. The parameters of the ANN used in the present case are presented in Table 3.

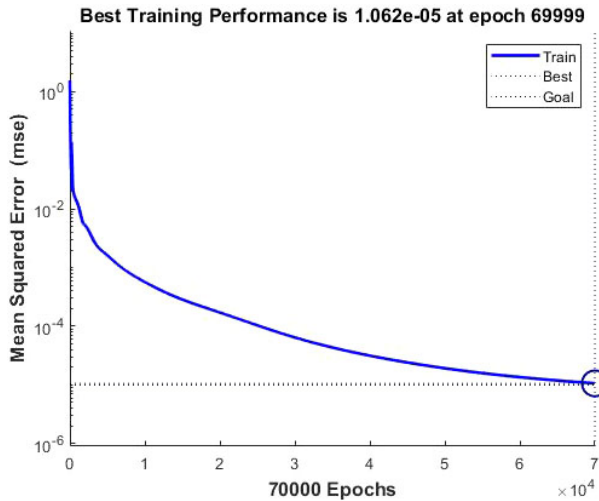


Fig. 8. ANN training performance.

Table 3. Parameters used in ANN.

S. No.	Parameters used in ANN training	Values
1	Network configuration	7-7-7-1
2	Number of neurons in the Input layer	7
3	Number of neurons in the output layer	1
3	Maximum number of epochs	70000
4	Goal (Mean Square Error)	0.00001
5	Activation functions for hidden and output layers	Tansig
6	Activation function for input layer	Logsig

## 5.2. Results of the ANN

The developed ANN model is evaluated using a new set of input values in order to establish its capability of predicting the gear faults. The predicted ANN results for the *new features* (NF) corresponding to the normal gear, worn-out tooth, broken tooth and broken tooth with load conditions are presented in Table 4. The new features used in the evaluation phase were not used in the training process.

It is evident from Table 4 that the fault classified by the ANN for the new input features was highly accurate as it made a close agreement with the actual results. Hence, the reliability of the integrated technique of the Hu invariant moments and the ANN is proven to be good and, as such, it can be applied to automated monitoring of gear faults.

Table 4. Effectiveness of gear fault classification by ANN.

S. No.	New Features (NF)	Gear Fault classification		
		Predicted by ANN	Actual fault	
1	NF1	0.1480	0	Normal gear
2	NF2	0.0185	0	Normal gear
3	NF3	0.0001	0	Normal gear
4	NF4	1.1958	1	Worn-out tooth
5	NF5	1.9040	2	Broken tooth
6	NF6	2.2072	2	Broken tooth
7	NF7	2.8571	3	Broken tooth under load
8	NF8	2.9048	3	Broken tooth under load
9	NF9	2.9910	3	Broken tooth under load

## 6. Conclusions

In the present work, the Hu invariant moments were successfully used to extract the nonlinear features from time-frequency signals of gears under non-stationary conditions. The ZAM transform was used to convert the signals from the time domain into the time-frequency domain. The ANN model was developed to automate the process of fault classification. The ANN was trained with fault features extracted by the Hu moments. Subsequently, the ANN was evaluated with new input features and the predicted results were compared with the actual gear faults. The prediction accuracy of the ANN was found to be 100% for identifying the gear faults with a new set of data. The deviation between the actual and the predicted results are within the range of 0.0001 to 0.2072 which is significantly small. The prediction accuracy was attributed to the successful fault feature extraction using the Hu invariant moments that are used to train the ANN. Further, the optimum structure of the ANN was also contributed in the classification of faults by improving the nonlinear capability of the ANN. Hence, the integrated technique of the ZAM transform, the Hu invariant moments-based feature extraction and the ANN was proven to be an effective tool in the automated gear fault detection. The presented approach is very viable in the industry if the data collection and the feature extraction are carried out at both the installation stage and the routine operation of the gears. Despite the effectiveness of the proposed approach in classifying the type of faults, there is a scope for extending the research to identify the combination of faults and the severity of faults in gears.

## References

- [1] Li, G., Fangyi, L., Haohua, L., Dehao, D. (2018). Fault Features Analysis of a Compound Planetary Gear Set with Damaged Planet Gears. *Proceedings of the Institution of Mechanical Engineers, Part C: Journal of Mechanical Engineering Science*, 232(9), 1586–1604.
- [2] Charley, J., Bodovillé, G., Degallaix, G. (2001). Analysis of Braking Noise and Vibration Measurements by Time-Frequency Approaches. *Proceedings of the Institution of Mechanical Engineers, Part C: Journal of Mechanical Engineering Science*, 215(112), 1381–1400.

- [3] Chaari, R., Mohamed, T. K., Maher, B., Fagher, C., Mohamed, H. (2016). Dynamic Analysis of Gearbox Behaviour in Milling Process: Non-Stationary Operations. *Proceedings of the Institution of Mechanical Engineers, Part C: Journal of Mechanical Engineering Science*, 230(19), 3372–3388.
- [4] Urbanek, J., Barszcz, T., Uhl, T. (2012). Comparison of advanced signal-processing methods for roller bearing faults detection. *Metrology and Measurement Systems*, 19(4), 715–726.
- [5] Zimroz, R., Urbanek, J., Barszcz, T., Bartelmus, W., Millios, F., Martin, N. (2011). Measurement of instantaneous shaft speed by advanced vibration signal processing – Application to wind turbine gearbox. *Metrology and Measurement Systems*, 18(4), 701–712.
- [6] Su, Z., Yaoming, Z., Minping, J., Feiyun, X., Jianzhong, H. (2011). Gear Fault Identification and Classification of Singular Value Decomposition Based on Hilbert-Huang Transform. *Journal of Mechanical Science and Technology*, 25(2), 267–272.
- [7] Krishnakumari, A., Elayaperumal, A. (2013). Application of Discrete Wavelet Transform and Zhao-Atlas-Marks Transforms in Non-Stationary Gear Fault Diagnosis. *Journal of Mechanical Science and Technology*, 27(3), 641–647.
- [8] Sun, R., Zhibo, Y., Xuefeng, C., Shaohua, T., Yong, X. (2018). Gear Fault Diagnosis Based on the Structured Sparsity Time-Frequency Analysis. *Mechanical Systems and Signal Processing*, 102, 346–363.
- [9] Zhang, X., Jianshe, K., Hongzhi, T., Jianmin, Z. (2015). A New Gerabox Fault Diagnosis Method Based on Lucy–Richardson Deconvolution. *Transactions of the Canadian Society for Mechanical Engineering*, 39(3), 593–603.
- [10] Afia, A., Chemseddine, R., Djamel, B. (2018). Gear Fault Diagnosis Using Autogram Analysis. *Advances in Mechanical Engineering*, 10(12), 1–11.
- [11] Guan, Y., Juanjuan, S., Ming, L., Dan-Sorin, N. (2019). Gearbox Fault Diagnosis via Generalized Velocity Synchronous Fourier Transform and Order Analysis. *Transactions of the Canadian Society for Mechanical Engineering*, 43(2), 153–163.
- [12] Juan, J.S., Miguel, D., Roque, A.O., Rene, D.J.R. (2018). Diagnosis Methodology for Identifying Gearbox Wear Based on Statistical Time Feature Reduction. *Proceedings of the Institution of Mechanical Engineers, Part C: Journal of Mechanical Engineering Science*, 232(15), 2711–2722.
- [13] Krishnakumari, A., Elayaperumal, A., Saravanan, M., Arvindan, C. (2017). Fault Diagnostics of Spur Gear Using Decision Tree and Fuzzy Classifier. *International Journal of Advanced Manufacturing Technology*, 89(9–12), 3487–3494.
- [14] Dhamande, L.S., Chaudhari, M.B. (2018). Compound Gear-Bearing Fault Feature Extraction Using Statistical Features Based on Time-Frequency Method. *Measurement*, 125, 63–77.
- [15] Zhang, C., Zhongxiao, P., Shuai, C., Zhixiong, L., Jianguo, W. (2018). A Gearbox Fault Diagnosis Method Based on Frequency-Modulated Empirical Mode Decomposition and Support Vector Machine. *Proceedings of the Institution of Mechanical Engineers, Part C: Journal of Mechanical Engineering Science*, 232(2), 369–380.
- [16] Vamsi, I., Sabareesh, G.R., Penumakala, P.K. (2019). Comparison of Condition Monitoring Techniques in Assessing Fault Severity for a Wind Turbine Gearbox under Non-Stationary Loading. *Mechanical Systems and Signal Processing*, 124, 1–20.
- [17] Saravanan, N., Ramachandran, K.I. (2010). Incipient Gear Box Fault Diagnosis Using Discrete Wavelet Transform (DWT) for Feature Extraction and Classification Using Artificial Neural Network (ANN). *Expert Systems with Applications*, 37(6), 4168–4181.
- [18] Wang, C.C., Yuan, K., Chin, C.L. (2013). Gear Fault Diagnosis in Time Domains via Bayesian Networks. *Transactions of the Canadian Society for Mechanical Engineering*, 37(3), 665–672.

- [19] Dworakowski, Z., Dziedziech, K., Jabłonski, A. (2018). A novelty detection approach to monitoring of epicyclic gearbox health. *Metrology and Measurement Systems*, 25(3), 459–473.
- [20] Rajagopalan, S., Restrepo, J.A., Aller, J.M., Habetler T.G., Harley, R.G. (2008). Non stationary motor fault detection using recent quadratic time-frequency representations. *IEEE Transactions on Industrial applications*, 44(3), 735–744.
- [21] Hlawatsch, F., Boudreaux-Bartels, G.F. (1992). Linear and quadratic time–frequency signal representations, *IEEE Signal Processing Magazine*, 9(2), 21–67.
- [22] Ming-Kuei, H. (1962). Visual Pattern Recognition by Moment Invariants. *IRE Transactions on Information Theory*, 8(2), 179–187.
- [23] Barreiro, J., Castejón, M., Alegre, E., Hernández, L.K. (2008). Use of Descriptors Based on Moments from Digital Images for Tool Wear Monitoring. *International Journal of Machine Tools and Manufacture*, 48(9), 1005–1013.